Spherulitic Nucleation and Growth Rates in an iPP under Continuous Shear Flow

I. Coccorullo, R. Pantani,* and G. Titomanlio

Department of Chemical and Food Engineering, University of Salerno, Via Ponte don Melillo, 84084 Fisciano (SA), Italy

Received July 8, 2008; Revised Manuscript Received October 14, 2008

ABSTRACT: The study of polymer crystallization enhanced by flow has attracted much interest because it implies the possibility of controlling the final morphology and the resulting mechanical and functional properties of semicrystalline polymers. An improved understanding of the fundamentals of flow-enhanced crystallization effects can help to tailor advanced processing strategies. Indeed, a complete understanding of the fundamentals of structure development during processing remains a challenge. In this work, the effect of a steady shear flow applied during crystallization on the morphology evolution and on the kinetics of isothermal crystallization of an iPP has been studied experimentally. In particular, measurements of nucleation and growth rates of spherulites during continuous and constant steady shear flow were performed by means of a Linkam shearing cell coupled with an optical microscope. During all the tests carried out in this work, the dominant crystalline structure was fully spherulitic. It was found that nucleation density in quiescent conditions remained constant with time (i.e., no nucleation rate was observed during the test). On the contrary, under shear flow, an increase of nucleation density with time was observed. This increase was found to be essentially linear with time. The linear dependence allowed to calculate a constant nucleation rate, which was found to be dependent on shear rate according to a power law expression whose exponent was found to be about 3. The evolution of crystallinity under shear conditions, calculated combining the results obtained on nucleation and growth rate, was also successfully compared with data obtained in the same conditions by means of in situ wide-angle X-ray diffraction. Finally, an attempt was made to determine scaling rules which can describe the effect of flow on crystallization kinetics.

Introduction

The reason for the intense interest in crystallization of flowing polymer melts, when even quiescent crystallization is not yet completely understood, is its immense technological relevance to polymer processing. Semicrystalline polymers comprise nearly two-thirds of all synthetic polymers. These are processed to form films, fibers, and molded articles using operations such as extrusion, molding, fiber spinning, film blowing, etc. During these processing operations, the polymer melt is subjected to complex and intense flow fields (shear, elongational, or mixed) during or soon after which the polymer crystallizes. The crystallization kinetics and the morphology of the semicrystalline polymer in the final product, and subsequently its properties and quality, depend upon the orientation of the melt by effect of the flow. The possibility of controlling the final morphology and the resulting mechanical and functional properties of semicrystalline polymers[1−16] based on the study of polymer melt crystallization stimulated by flow is highly intriguing.

By changing the processing conditions (temperature, strain rate) and molecular parameters, a wide range of molecular morphologies, such as spherulites, shish-kebab or row-nucleated structures can be produced which opens up the possibility of tailoring desired microstructures.

An improved understanding of the fundamentals of flow-enhanced crystallization effects can help to tailor advanced processing strategies which are guided by a better insight into the interplay between macromolecular flow dynamics and polymer crystallization.

Generally, it is considered that flow (which in most of processes essentially means shear) enhances crystallization rate. Crystallization, in the above context, includes both nucleation and growth. The phenomenon of flow induced crystallization is attributed mainly to the orientation of crystallizable polymer chains in the melt under shear conditions. The effect of flow is certainly large on the nucleation step.[17−24] Nucleation, under a given set of conditions, depends on the change of the free energy difference between the crystal and the melt phases. Since the degree of order in the melt phase increases under shear conditions, the free energy difference increases. Thus, the nucleation rate increases. On the other side, flow effects on the crystallization growth step are quite complex and were found not always as pronounced as those on the nucleation step.[23−26]

State of the Art on Rheo-optical Studies. In the last few decades, several investigations have been conducted on the effect of flow on the crystallization of a polymer melt, subjected to flow and a certain degree of undercooling. The interest into this problem was recently renewed because of the availability of new experimental tools that, coupled with advances in modeling and simulations, are beginning to yield insights into the molecular characteristics that control the crystallization pathways adopted by a stressed polymer melt. Most of the studies have concentrated on shear flow, which will also be the focus of this paper. It is now well-known that applying shear flow to an undercooled polymer melt enhances the crystallization process. The extent of this enhancement depends on many factors, such as the processing parameters and the molecular characteristics of the polymer.

The focus of early works in this field was placed essentially on the investigation of the overall crystallization kinetics[27−32] and the changes in the induction times during isothermal crystallization.[33] It has been shown that both these factors are considerably enhanced by the flow. It has been suggested that the main effect of flow is the modification of the nucleation process and the resulting change in the nucleation density. Under certain conditions, however, even the morphologies will change as a consequence of the experienced flow-induced molecular deformations. This effect occurs in the form of the change of

* To whom correspondence should be addressed. Tel.: +39089964141. E-mail: rpantani@unisa.it.

10.1021/ma801524t CCC: $40.75
Published on Web 11/12/2008

the typical spherulite shape encountered under quiescent conditions to oriented crystalline structures, such as shish-kebab or row-nucleated structures. Additionally, it has been shown that flow can also affect crystal growth kinetics.[23−26]

Despite the high relevance of these papers, to further improve our understanding of the crystallization process from a fundamental point of view, measurements of nucleation and of spherulites growth rate under shear are still needed. To this purpose, many recent papers deal with the "short-time shearing" protocol, developed by Janeschitz-Kriegl and co-workers.[29−34] This procedure allows to obtain a measure of nucleation and growth rate of spherulites after the application of a shear deformation. Many of the reported results have been obtained in the low shear rate region, using either rheometrical equipment or using commercial shear cells such as for instance the Linkam CSS-450. These studies have clearly demonstrated the enhancement of overall crystallization by effect of the preshear treatments.[8,14−18,21,22,35]

As underlined above, most of the literature works are focused on the nucleation and on the growth rates of spherulites only after the application of the shear. Only Wassner and Maier[17] studied the influence of shearing during isothermal crystallization experiments of iPP by rotational rheometry in combination with optical microscopy coupled with an optical shear cell. They observed that under quiescent condition the nuclei are all formed at the beginning of the isothermal experiments and no further nucleation occurs later during the experiment. The structure development is completely different if the crystallization occurs under high shearing as the number of nuclei increases tremendously during the crystallization process. These authors analyzed the effect of shear rate on the time scale of the crystallization, however their analysis was just qualitative: they did not quantitatively analyze the nucleation and the growth of the spherulites. Despite of the huge effort spent, the description of the evolution of morphology in shear conditions is thus still challenging. If an understanding of the fundamentals of structure development during processing is sought, additional experimentation of nucleation density and growth rate of spherulites during steady shear flow cannot be avoided.

In this work, the effect of a steady shear flow applied during crystallization on the morphology evolution and on the kinetics of isothermal crystallization of an iPP has been studied experimentally. In particular, an effort was made to obtain quantitative measurements of nucleation and, above all, growth rates of spherulites during continuous and constant steady shear flow. The measurements were performed by means of a Shear Linkam Cell coupled with an optical microscope. The evolution of crystallinity under shear conditions, calculated combining the results obtained on nucleation and growth rate, was also compared with data obtained in the same conditions by means of in situ wide-angle X-ray diffraction performed in the A2 beamline at the Hamburger Synchrotronstrahlungslabor at the Deutsches Elektronen-Synchrotron in Hamburg (Germany).[36−42]

Finally, an attempt was made to determine scaling rules which can describe the effect of flow on crystallization kinetics.

Experimental Section

Material. In this work, a commercial grade iPP resin (T30G, M_w = 481000, M_n = 75000, tacticity = 87.6%mmmm), kindly supplied by Montell (Ferrara, Italy), was adopted for the experiments. This material is the same as adopted by Titomanlio and co-workers to identify a model of crystallization kinetics able to describe morphology evolution under high cooling rate and pressure in quiescent conditions.[43−46]

Experimental Procedures. *Measurements of Spherulitic Nucleation Density and Growth Rate.* The observation of morphology and the measurement of nucleation density and growth rate under both steady shear and quiescent conditions were performed by means of a polarized light microscope (Olympus BH-41), equipped with a shearing cell (Linkam shearing cell, CSS450). Photographs were taken by a 3CCD color video camera. Samples were loaded between the top and bottom of deeply cleaned quartz windows, which were in thermal contact with silver block heaters. The shear effect and thermal treatment were imposed by the Linkam shearing cell. Steady shear was applied to the samples by rotation of the bottom quartz window at a constant velocity. Although the plate-plate geometry of the cell imposes different shear rates along the radial direction, a constant shear rate in the observation field can be obtained by locating the observation field at a fixed radial position (7.5 mm, in this case). Accordingly, the shear rate at the measurement point (window) was constant during any steady shear experiment. At this position, the accuracy of thermal control was checked by independent tests carried out by a thermocouple. Since the imposed shear rate depends on the thickness of the sample, after any test conducted by the Linkam shearing cell the thickness of the solidified sample was accurately measured. The test was considered valid, and thus the results were analyzed, only if the measured thickness was found to be consistent with the thickness imposed by the shearing device.

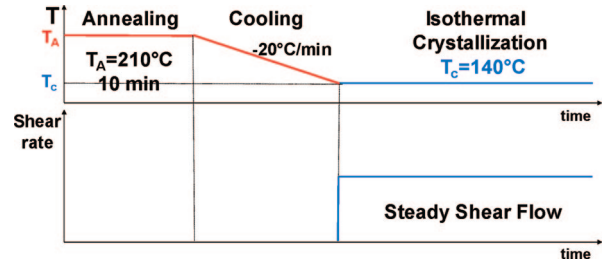

Figure 1. Thermo-mechanical protocol adopted for the crystallization experiments.

The isothermal crystallization of iPP resins (at T = 140 °C) was carried out under both quiescent and shear conditions. Polymer films with a thickness of about 200 μm were prepared, starting from pellets, by compression molding at T = 210 °C. Disks were cut from these films, they were inserted into the Linkam cell, heated and melted at T_m = 210 °C. Their thickness was reduced to 100 μm by slowly lowering the upper glass plate of the Linkam device. Subsequently, the sample was kept under these conditions at constant temperature for 10 min to erase previous thermal and mechanical history.

The microscope was focused on the central position between top and bottom windows, this focus position was chosen with the aim of minimizing wall effects on the crystallization. The temperature was then lowered at the rate of 10 °C/min until it reached the desired crystallization temperature of 140 °C. Zero time was assigned to the instant at which the crystallization temperature was reached. Shear flow was then applied at the chosen shear rate and images were acquired by the digital camera.

Test temperature was chosen so as to determine measurable characteristic crystallization times. In fact, too high temperatures (close to the thermodynamic melting temperature) resulted in very low crystallization rates, whereas too low temperatures caused an essentially instantaneous crystallization. In both cases, the measurements become impossible, or at best unreliable.

The thermo-mechanical protocol adopted for the crystallization experiments is described in Figure 1 and the experimental conditions are reported in Table 1.

Analysis of the Images. To analyze the micrographs collected during the crystallization process under shear, a software was developed in Labview (National Instruments). The developed software improves the contrast of the images by applying some digital filters, automatically identifies the elements in the micrographs and evaluates their number, their position and their dimension and finally it stores the collected information in a file. The

Table 1. Experimental Conditions Adopted in the Crystallization Experiments

annealing temp (T_A) [°C]	crystallization temp (T_c) [°C]	shear rate [s^{-1}]
210	140	0
210	140	0.07
210	140	0.11
210	140	0.15
210	140	0.175
210	140	0.20
210	140	0.25
210	140	0.30
210	140	0.50[a]
210	140	1.00[a]

[a] Only X-ray analysis.

reliability of the software was checked on a number of selected images on which the analysis was conducted manually.

During the crystallization process, the elements showed in the micrographs move increasing in number and dimensions because of the application of the shear. Therefore, the number of the nuclei could be followed and their dimension could be monitored as long as they remained inside the observation window that is in a time period which depended on the test but was always longer than about 30 s.

The evolution of the spherulite number and dimensions could be attained by applying the developed software for the image analysis to the series of micrographs collected during the crystallization under shear. In order to obtain reliable values of the spherulites nucleation density and growth rate a huge number of micrographs were collected during the crystallization and carefully analyzed. In particular, concerning the evolution of spherulitic radius, different spherulites were measured at different times from the beginning of the test, so that the growth rate could be measured, although on different spherulites, during the whole test time.

Measurements of Crystallinity Evolution. Measurements of the crystallinity evolution during steady shear flow were carried out in the A2 beamline at the Hamburger Synchrotronstrahlungslabor HASYLAB at the Deutsches Elektronen-Synchrotron DESY in Hamburg (Germany). The wavelength, λ, of X-ray beam was 0.15 nm for WAXD experiments. A 2D MARCCD detector was employed for the detection of 2D WAXD patterns. The detector resolution was set at 1024 × 1024 pixels. The Linkam stage was placed perpendicular to the incident X-ray beam. The aperture hole in the top window of the shear stage was aligned with the incident X-ray beam. The polymer melt was viscous enough to avoid any leakage even when the Linkam stage was mounted in the vertical position.

A photograph taken in the A2 beamline representing the shear cell placed between the source of the X-ray beam and the detectors is reported in Figure 2.

The experimental protocol adopted for the X-ray measurements was the same adopted for measurements of nucleation density and growth rate of spherulites and the experimental conditions are reported in Table 1. The X-ray pattern of the amorphous melt was collected immediately after the temperature reached the designated crystallization temperature, before the shear was applied. During the shear, 2D SAXS and WAXD patterns were collected continuously starting with the application of shear. At the end of the isothermal step, the sample was cooled to room temperature. One X-ray pattern of the sheared sample was also collected at room temperature. All X-ray data were corrected for background (air and instrument) scattering before analysis.

Differently from optical measurements, XR measures conducted at DESY were carried out by adopting aluminum-kapton plates. It was thus possible to keep shearing until complete crystallization (which is obviously not possible when using quartz plates which can break when material viscosity increases).

Results

Rheological Measurements. The rheological characterization of the material at the temperature of 140 °C is reported in Figure 3. The reported values represent a mastercurve at 140 °C of a combination of dynamic sweep tests carried out by a rotational rheometer and constant shear rate measurements performed by a capillary rheometer in the temperature range from 160 to 240 °C. It can be noticed that the material shows a shear thinning behavior even at the lowest applied deformation rates. This means that the characteristic relaxation time at 140 °C is at least of the order of 100s of larger. Coppola et al., who worked on the same material adopted in this work, report a maximum relaxation time at 140 °C of 88 s.[12] This means that, even at the lowest applied shear rates adopted in this work, namely 0.07/s, the Weissemberg (or Deborah) number based on the maximum relaxation time should be fairly larger than 1 and, thus, the flow should be effective in orienting the molecules.

Quiescent Crystallization. In this work, to obtain a reference state for the flow experiments, quiescent crystallization experiments were performed. The morphology, the nucleation density, and the growth rate of the spherulites were monitored during experiments performed under quiescent condition with the same thermal history of the shear flow experiments (Figure 1).

Four micrographs collected during the crystallization experiments performed in quiescent conditions were reported in Figure 4. Nucleation density was determined by counting the number of nuclei in the sample and growth rate was determined by measuring the diameter of spherulites as a function of time until impingement took place.

Experimental determinations showed that, consistently with literature indications for the adopted material,[47] nucleation resulted to be predetermined under quiescent condition: a fixed number of nuclei appeared at the test temperature, and their number did not change in time. Furthermore, spherulite radius growth rate was found constant with time.

Results of growth rate and nucleation density, evaluated in quiescent condition at $T = 140$ °C are reported in Table 2; these values nicely compare with literature results obtained on the same polypropylene,[43] adopting the same conditions but a different device.

Crystallization under Shear Flow. The typical effects of the flow on the morphology evolution observed during crystallization tests are shown in Figure 4 where micrographs collected during the crystallization process under shear condition ($\dot{\gamma} = 0.175$ s^{-1} and $T = 140$ °C) are reported. The first effect arising from the applied shear is the increase in the nucleation density with time: experimental data show that under flow the number of activated nuclei increases during the test, whereas under quiescent conditions for the resin analyzed it was function of temperature only. This effect is confirmed by the heterogeneity of the spherulites dimensions: in fact, nuclei generated at different times show different dimensions.

Under the experimental conditions adopted in this study, the morphology under shear maintained the spherulitic structure, as shown in Figure 5. This structure is dominant also after the application of the shear for long periods, when the spherulites fill most of the space. This is shown in Figure 6, where micrograph collected after about 600 s of application of the shear (shear rate 0.30 s^{-1}) is reported.

Effect of the Shear Rate. The effects of the intensity of the shear flow on the morphology of the spherulitic structure during crystallization at $T = 140$ °C are shown in Figure 7 where optical micrographs collected during crystallization process under different shear rates ($\dot{\gamma} = 0.11$ and 0.175 s^{-1}) are reported. Both of the micrographs were collected after 2000 s from the time at which temperature reached the isothermal crystallization temperature and shear started. Figure shows that the number of nuclei after a given time strongly increases on increasing the shear rate.

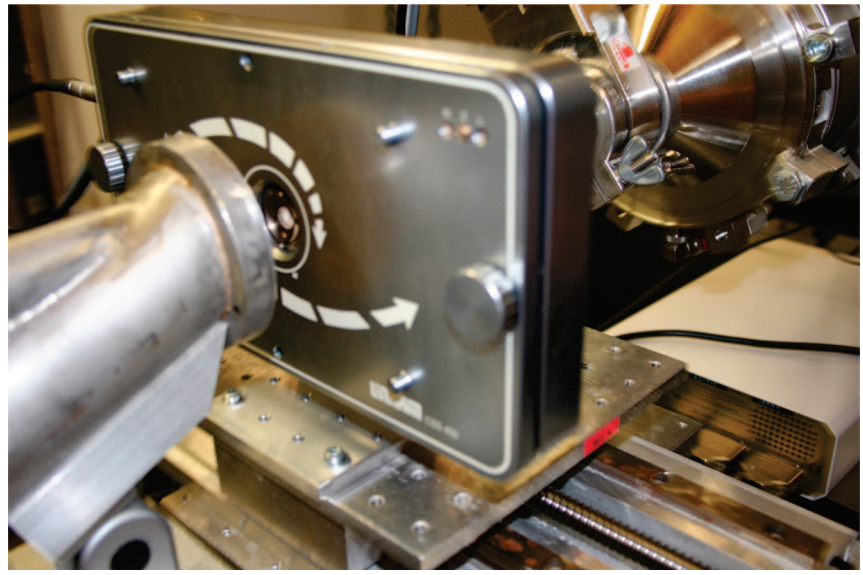

Figure 2. Placement of the shear cell in the X-ray beam line.

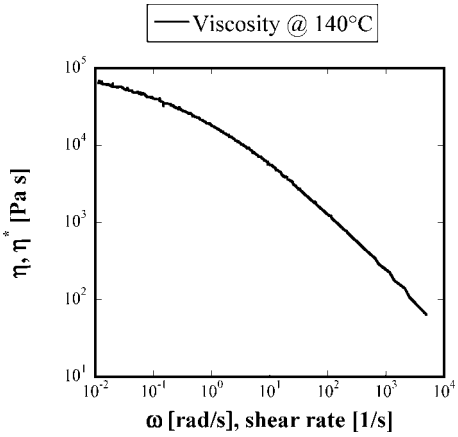

Figure 3. Rheological characterization of the material at the temperature of 140 °C.

Nucleation Density Measurements. The evolution of the nucleation density during the crystallization under shear, evaluated by means of the image analysis software, is reported in Figure 8 for all the test performed in this work. Data reported in Figure 8 confirm that under flow conditions the number of activated nuclei increases with time, whereas under quiescent conditions for the resin analyzed it was function only of temperature and that the number of nuclei strongly increases on increasing the shear rate.

Figure 8 also shows that nucleation density increases about linearly with time. Janeschitz-Kriegl[7,19] suggests a power law dependence of the nucleation density with time. The data reported in this work are not incompatible with such a dependence, but the exponent of power-law is very close to 1 (ranging from 0.8 to 1.3).

The simplest dependence for the evolution of the nucleation density suggested by Figure 8 can be expressed by eq 1

$$N(t,\dot{\gamma}) = N_0 + \dot{N}(\dot{\gamma}) \times \mathrm{t} \tag{1}$$

where $N(t, \dot{\gamma})$ is the evolution of the total number of nuclei, $\dot{N}$ is the nucleation rate which depends on the shear rate and N_0 is the number of the nuclei generated when temperature reaches the isothermal crystallization temperature ($t = 0$ s).

Eq 1 keeps into account the experimental evidence that commercial polymers like the one adopted in this work present a heterogeneous nucleation in quiescent conditions. Homogeneous nucleation can also be present, but it is overcome by the other mechanism in quiescent conditions. On the contrary, homogeneous nucleation can be enhanced by flow and becomes a competing, or even overcoming, mechanism.[48]

Indeed, a careful analysis of data reported in Figure 8 shows that for some of the tests, especially the ones carried out at the lowest shear rates, the linear interpolation intercepts the time axis at positive values of time (of the order of 100 s), indicating a delayed nucleation. However, this cannot be assumed as a significant proof of the existence of an induction time. There are indeed some sources of uncertainties that do not allow an accurate measurement of the nucleation start: (I) some time is needed to reach a steady orientation inside the sample, and (II) a spherulite can be detected only when its diameter is of the order of 1 μm and, thus, the time at which it is generated can be measured only by estrapolation, which induces itself uncertainties. Both the indicated reasons are of the right order of magnitude to justify a nonzero intercept in the plots of Figure 8. The values of nucleation rate obtained by a linear fitting of the evolution of nucleation density for all the shear rates applied in this work, were reported as a function of the shear rate in Figure 9. These data, consistently with indication of Figure 8, show that nucleation rate increases on increasing the shear rate. Moreover, the data seem to indicate that nucleation rate increases exponentially with shear rate. As expected on the basis of the high Weissemberg number, the effect of shear rate is significant also at the lowest applied shear rate. Indeed, Coppola et al. indicated that for this polymer the critical shear rate below which the effect of flow does not affect crystallization rate at 140 °C is 0.048/s, namely, smaller than the minimum shear rate adopted in this work.[12]

Growth Rate Measurements. In the literature, many papers deal with the effect of shear flow on the nucleation step and most of the authors agree on the enhancement of the nucleation rate due to the flow. In comparison, little is known about the effect of shear on the crystal growth rate and, moreover, there is not an unanimous consensus of opinion about this topic.[23−26]

As already reported, the software for image analysis is able to identify the spherulites in the micrographs and to evaluate their dimensions. During the crystallization tests under shear spherulites move increasing in dimensions then the spherulitic growth rate can be evaluated by monitoring their dimension as long as they remain inside the observation window.

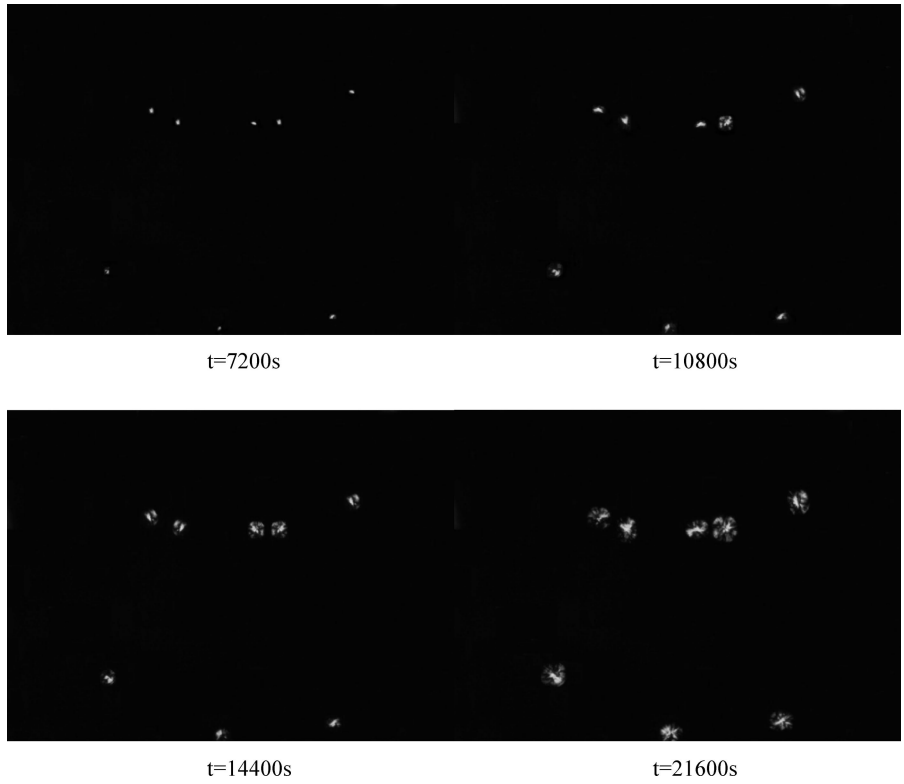

Figure 4. Micrographs collected during the quiescent crystallization tests at 140 °C.

Table 2. Results of Growth Rate and Nucleation Density in Quiescent Condition at $T = 140$ °C

quiescent conditions ($T = 140$ °C)	
nucleation density	7.0×10^{-8} nuclei/μm^3
growth rate	0.008 μm/s

In Figure 10 the evolution of the radius of a spherulite during crystallization under shear ($\dot{\gamma} = 0.11$ s^{-1}) is reported. Data show that the radius increases linearly with time, and thus that the growth rate of the spherulites is constant at least in the laps of time in which they remain inside the observation window. To evaluate the evolution of the spherulitic growth rate during the shear crystallization tests, this analysis was performed on a broad number of spherulites for different crystallization times. To minimize measurement error, only the diameters of clearly defined spherulites were measured. Results of this analysis show that spherulitic growth rate is almost constant during the whole crystallization process.

Values of spherulitic growth rate, obtained by a linear fitting of the evolution of spherulites dimensions for all shear rates applied in this work, were reported as function of the shear rate in Figure 11. The spherulitic growth rates under shear conditions are always higher than that in the quiescent state.

Figure 11 shows that at the same crystallization temperature, as the shear rate increases in the range analyzed in this work, the spherulitic growth rate increases exponentially.

X-ray Analysis. Figure 12 shows representative two-dimensional WAXD patterns collected during the crystallization experiments performed under shear flow ($\dot{\gamma} = 0.30$ s^{-1}). The initial X-ray scattering patterns show diffuse rings representing scattering from an isotropic melt. As crystallization proceeds, discrete reflections appear over the diffuse halo. These reflections can be indexed as the (110), (040), (130), (111), and (131) of the α-monoclinic form of iPP.[49]

Circularly averaged WAXD intensity profiles were extracted from the 2D images for the evaluation of the crystallinity index.

In Figure 13, the WAXD intensity patterns as a function of time collected during quiescent crystallization are compared with the ones collected during shear crystallization ($\dot{\gamma} = 1$ s^{-1}).

In the quiescent crystallization test, the initial X-ray scattering patterns show only the diffuse halo representing scattering from an isotropic melt. As crystallization proceeds, peaks appear over the diffuse halo. These peaks can be indexed as the (110), (040), (130), (111), and (131) characteristic of the α-monoclinic form of iPP. Figure 13 underlines the effect of flow on crystallization kinetics: in fact, the same behavior can be observed also in the shear crystallization test, but the time scale is very different since in the quiescent crystallization test peaks are detectable after about 1000 s, whereas in shear crystallization test after 1000 s the sample appears to be fully crystallized.

In Figure 14 the evolution of the WAXD intensity patterns collected during shear crystallization test $\dot{\gamma} = 1$ s^{-1}) is magnified. In the figure there is evidence of a reflection at the equator around $2\theta = 16.8°$, indicating a small presence of β-phase in the sample (marked in figure). Measurements carried out at lower shear rates did not show the presence of beta phase. It can be thus inferred that during the tests carried out by the Linkam Shearing Cell, alpha phase is the only crystalline phase that develops.

A peak-fitting software was used to discriminate the crystalline peaks from the amorphous phase halo in the intensity profiles.[50] The total crystallinity index was determined after subtraction of the amorphous contribution in the total intensity profile. The overall crystallinity, X_c, was thus calculated by

$$X_c = \frac{\Sigma_i A_{cryst}}{\Sigma_i A_{cryst} + \Sigma_i A_{amorp}} \quad (2)$$

where A_{cryst} and A_{amorp} are the fitted areas of crystal and amorphous, respectively. Obviously, deconvolution results are affected by some uncertainty, it was estimated as ±3% on the percentage of crystalline phase.

In Figure 15, the values of the overall crystallinity index X_c obtained by the deconvolution are reported as symbols versus

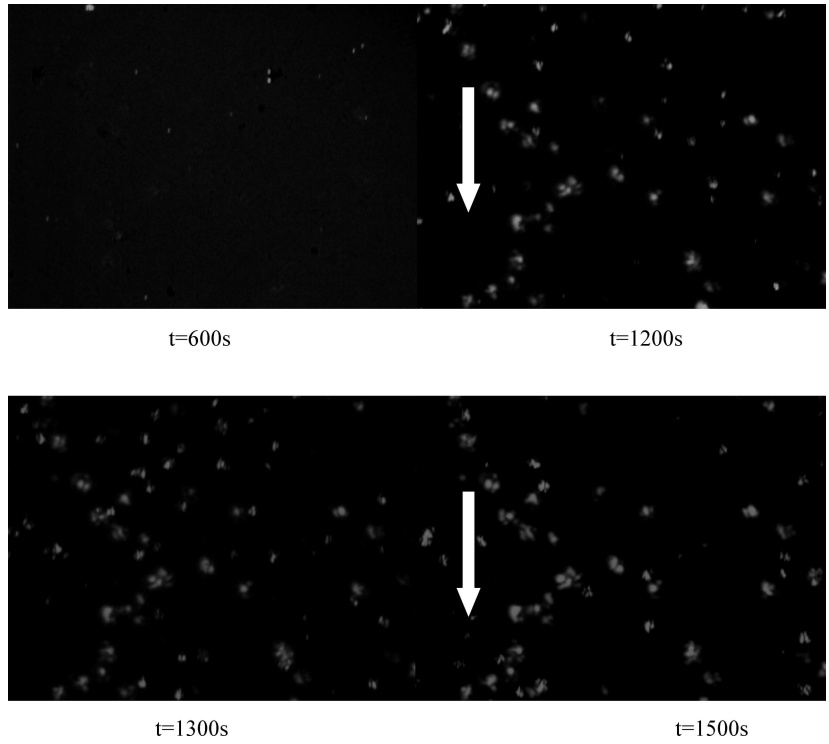

Figure 5. Micrographs collected during crystallization process under shear condition ($\dot{\gamma} = 0.175$ s^{-1} and $T = 140$ °C). Flow direction is also indicated in figure.

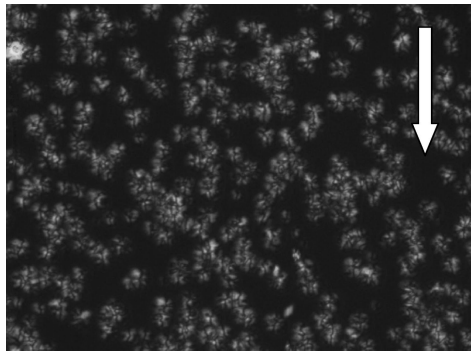

Figure 6. Micrograph collected during crystallization process under shear condition ($\dot{\gamma} = 0.30$ s^{-1}, $t = 600$ s and $T = 140$ °C). Flow direction is also indicated in figure.

the shearing time for some crystallization test performed at Hamburger Synchrotronstrahlungslabor (HASYLAB). The enhancement of the crystallization rate due to the application of the flow is evident. In fact, as expected, crystallization kinetics become faster upon increasing the shear rate applied.

To calculate the evolution of crystallinity under shear conditions, values of nucleation and growth rates evaluated in this work were combined and results were compared with the evolution of crystallinity evaluated by means of two-dimensional WAXD.

Adopting the equation of Avrami, the evolution of crystallinity can be calculated as[29]

$$X_c = 1 - \exp[-K_\alpha(t)] \tag{3}$$

where K represents the volume of the crystallinity fraction. Kolmogoroff equation was adopted in this work to describe the evolution of the volume fraction crystallized toward α form[29]

$$K_\alpha = \frac{4}{3}\pi \int_0^t \left(\dot{N}(s)\left(\int_s^t G(r)\, dr\right)^3\right) ds \tag{4}$$

Eq 4 describes a spherical growth of crystalline entities, like that observed in all the experiments carried out in this work. The values of nucleation rate and growth rate of spherulites evaluated in this work were adopted to calculate the evolution of crystallinity during shear experiments. Results of the evolution of crystallinity calculated from results of nucleation and growth rate (reported in Figure 15 as lines) nicely compare with values calculated from the deconvolution of the WAXD intensity profile. As mentioned above, the Linkam shearing cell could not be operated with transparent plates until complete crystallization was attained. In Figure 15, the maximum time for which each test was conducted was marked by a vertical segment. Nevertheless, the results obtained for growth rate were kept valid in eq 4 also for a longer time.

A series of conclusions can be drawn from the comparison reported in Figure 15: (1) Eq 4 is able to describe the evolution of crystallinity also in sheared samples (once correct evolutions are assumed for nucleation rate and spherulitic growth rate) until complete crystallization is attained. (2) The evolutions of nucleation rate and spherulitic growth rate, found by tests in which crystallinity did not reach its ultimate value, could be extrapolated to describe tests during which shear was kept until fully crystalline samples were obtained (as done at DESY).

Discussion

Most of the research groups working in the area of polymer processing made an independent choice regarding the description of the flow induced crystallization phenomenon. Essentially, the attitude of the researchers was to optimize the description of a particular set of experimental data, trying to relate the enhancement factors to an easily accessible variable: from the simplest possible choice which is obviously the shear rate, to a choice based on more sound physical basis, namely, the stress tensor, and to probably the best option which is based on energy (or entropy) functions. It is, however, still under discussion which variable is the most suitable to describe the effect of flow on crystallization kinetics and morphology evolution.

In our opinion, the only path to successfully approach the problem of morphology evolution under flow is to obtain fully

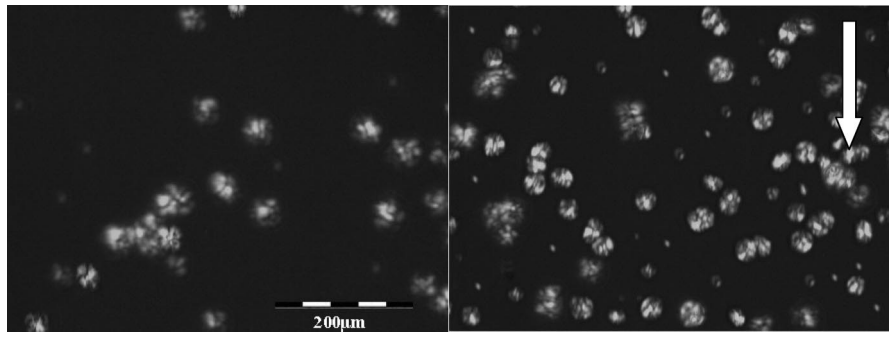

Figure 7. Micrographs collected during crystallization under different shear rates ($\dot{\gamma}$ = 0.11 s^{-1}, left, and 0.175 s^{-1}, right, t = 2000 s). Flow direction is also indicated in figure.

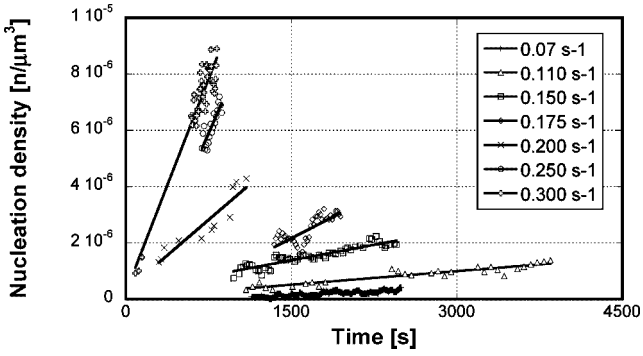

Figure 8. Evolution of nucleation density under steady shear flow (T = 140 °C).

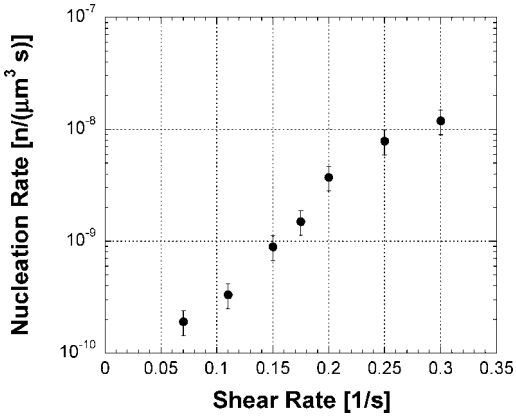

Figure 9. Nucleation rate obtained by a linear fitting of the evolution of nucleation density data (T = 140 °C).

characterized sets of data on a material whose behavior is known at the best of current knowledge in the widest possible range of conditions. This paper moves along this direction.[43−46]

In the literature, a number of mathematical models of the effects of the flow on crystallization of polymers can be found. A schematization of the models proposed in the literature can be found in the papers by Tanner and Qi[51] or Pantani et al.[45] In the following, some variables are considered for the description of the effect of flow on crystallization kinetics and an attempt is made to determine the variable which is more adequate to describe the effect of flow on crystallization kinetics.

Shear Rate. The research group of Janeschitz-Kriegl[5] let nucleation rate be proportional to $(\dot{\gamma}/\dot{\gamma}_c)^p$, where p and $\dot{\gamma}_c$ are unknown constants. They have suggested such a form with p = 2 for higher shear rates. Figure 16 shows that, to obtain the best fitting of the experimental data collected in this work, a value of about 3 is needed.

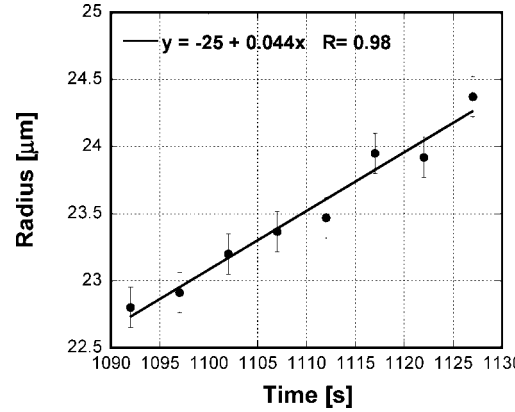

Figure 10. Evolution of spherulite dimensions during crystallization under shear ($\dot{\gamma}$ = 0.20 s^{-1} and T = 140 °C).

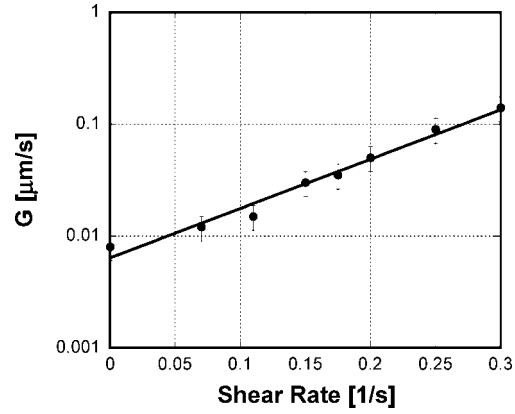

Figure 11. Spherulitic growth rate, obtained by a linear fitting of the evolution of spherulite dimensions for each shear rate applied in this work, as function of the shear rate (T = 140 °C).

A parameter which is often adopted to describe the effect of flow on crystallization is the Deborah (or Weissemberg) number.[52] Indeed, for our experimental conditions in which the temperature is kept constant and the shear rates range within the same order of magnitude, a plot of nucleation rate versus Deborah number would be quite similar to the plot reported in Figure 16.

Nucleation Rate and Spherulitic Growth Rate: The Undercooling. As shown above, both nucleation and growth rates depend on shear rate. In Figure 17, we report a diagram that relates the nucleation rate with the spherulitic growth rate at the same shear rate.

The results reported in Figure 17 clearly indicate that, under flow conditions, the increases of nucleation rate with respect to

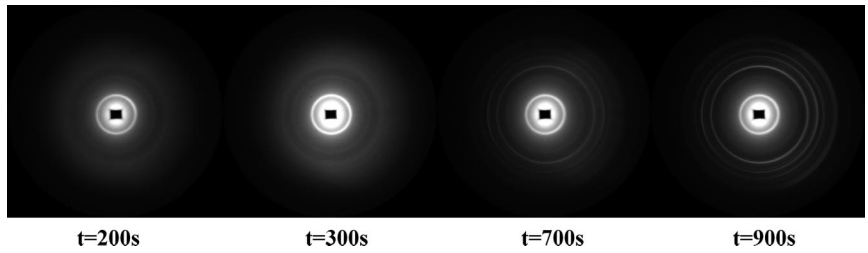

Figure 12. Two-dimensional WAXD patterns collected during the crystallization experiments performed under shear flow ($\dot{\gamma} = 0.30\ s^{-1}$).

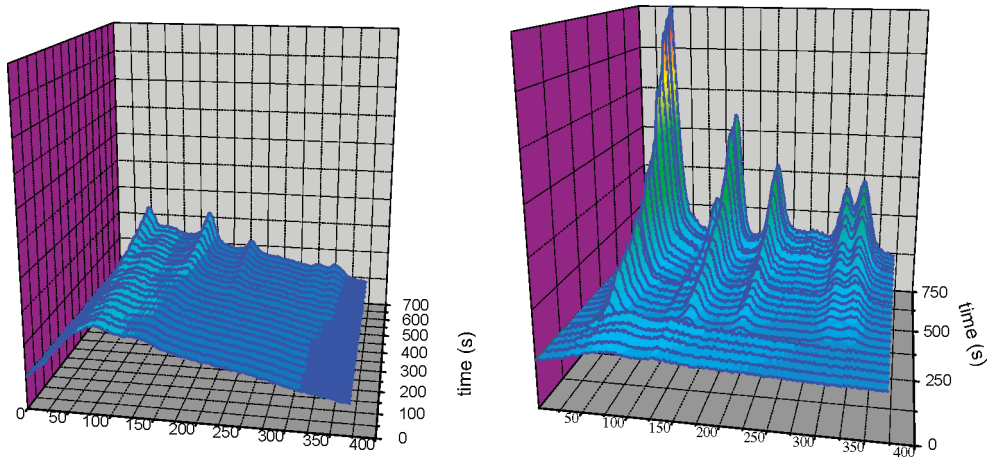

Figure 13. WAXD intensity patterns as a function of time collected during quiescent and shear crystallization ($\dot{\gamma} = 1\ s^{-1}$).

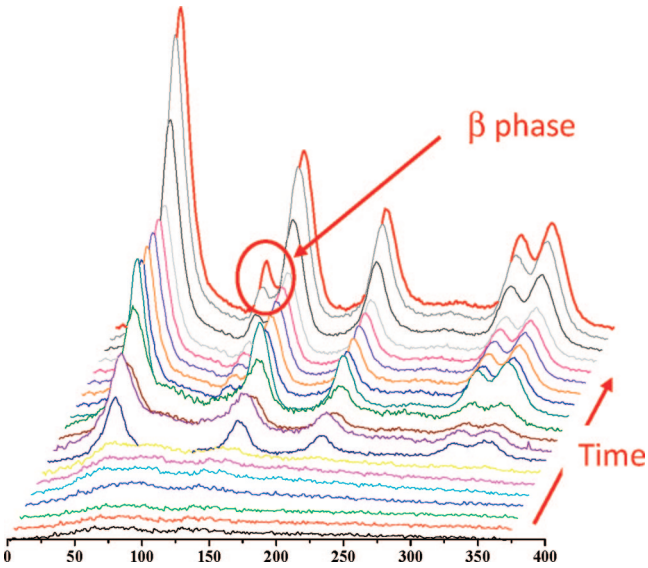

Figure 14. Evolution of the WAXD intensity patterns collected during shear crystallization test ($\dot{\gamma} = 1\ s^{-1}$).

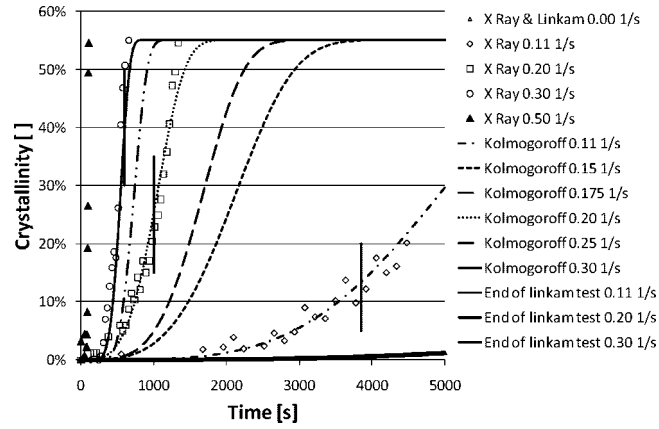

Figure 15. Evolution of the overall crystallinity index X_c as a function of the shearing time for some crystallization test performed at Hamburger Synchrotronstrahlungslabor (HASYLAB). Vertical segments identify the end of Linkam optical tests.

quiescent conditions are about proportional to the increases of the spherulitic growth rate.

The idea guiding many of the papers on the effect of flow on crystallization kinetics was focused on the changes of the melting temperature due to the flow. In fact, the melting point increases because of an entropy decrease due to the flow induced chain extension in the melt and the increase in melting temperature goes together with earlier and faster crystallization.[19]

In this work, the increase of the melting temperature was evaluated on the basis of experimental data of growth rate of spherulites. Indeed, according to the results obtained in a previous work,[43] at different temperatures under quiescent conditions on the same material adopted in this work, the temperature dependence of the growth rate can be successfully expressed by the following equation[53]

$$G[T] = G_0 \exp\left[-\frac{U}{R\cdot(T-T_\infty)}\right] \exp\left[-\frac{K_g\cdot(T+T_m)}{2T^2\cdot(T_m-T)}\right] \quad (5)$$

and all the parameters appearing in eq 5 were identified.

Assuming that the values of the constants G_0, T_∞, U, and K_g do not depend on the flow conditions, once the value of $G(T)$ under flow is measured, the only unknown parameter in eq 5 is the flow induced melting temperature T_m. The values of the melting temperature for each shear rate which should be substituted in eq 5 to obtain the results of growth rate reported in Figure 11 are depicted in Figure 18 for all the tests conducted in this work.

The results show that the imposed shear flow leads to an increase of the melting temperature as high as 10 °C. This means

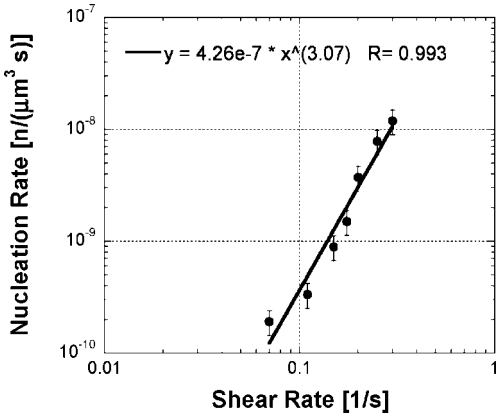

Figure 16. Nucleation rate obtained by a linear fitting of the evolution of nucleation density data analyzed in terms of shear rate.

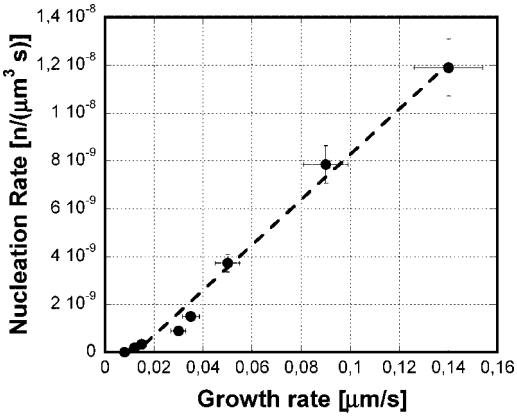

Figure 17. Nucleation rate vs the spherulitic growth rate under flow conditions.

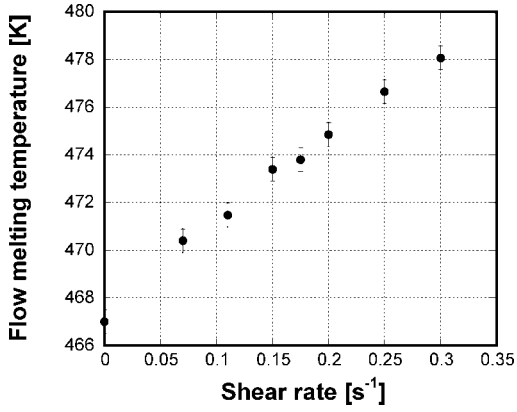

Figure 18. Increase in melting temperature due to the effect of flow.

that the undercooling (namely the difference between the melting temperature and the test temperature) increases of the same amount on increasing the shear rate. In Figure 19, the experimental values of nucleation rate are plotted against the inverse of the undercooling. This last choice was made because the inverse of the undercooling appears in the eq 5. Figure suggests that nucleation rate, at least for the isothermal tests carried out in this work, is an exponential function of the undercooling (or of its inverse).

Conclusions

In this work, a series of isothermal crystallization tests were conducted on an iPP, by imposing different shear rates, ranging from zero (quiescent conditions) to 0.3 s^{-1}, which were kept constant during the whole test. The history of crystallization for each test was monitored by means of two methods: direct observation of nucleation density and growth rate by means of optical micrographs and X-ray diffraction patterns collected at DESY.

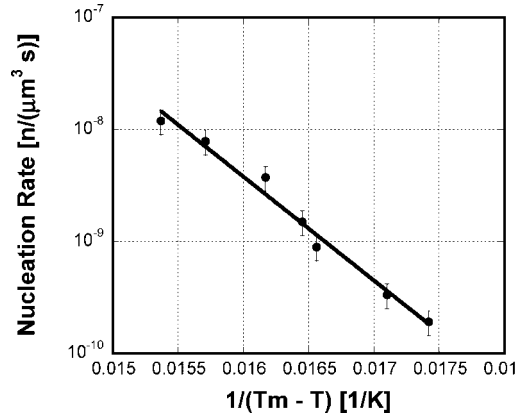

Figure 19. Nucleation rate, obtained by a linear fitting of the evolution of nucleation density data, analyzed in terms of undercooling.

During all the tests carried out in this work, the dominant crystalline structure was fully spherulitic. It was found that nucleation density in quiescent conditions remained constant with time (i.e., no nucleation rate was observed during the test). On the contrary, under shear flow, an increase of nucleation density with time was observed. This increase resulted to be essentially linear with time. The linear dependence allowed to calculate a constant nucleation rate, which was found to be dependent on shear rate according to a power law expression, whose exponent was found to be about 3.

During the same tests, it was also possible to collect data of spherulitic radius increase. It was found that the growth rate is essentially constant during the test (both in quiescent and flow conditions), and that it is an increasing function of shear rate. This result sheds some light on the controversial effect of flow on spherulitic growth rate.

It was found that the effects of flow on nucleation rate and on the increase of growth rate are just proportional to each other.

The experimental data of nucleation rate and spherulitic growth rate were substituted in the Kolmogoroff equation for the description of crystallization kinetics under isothermal conditions. The results were compared with the experimental data collected at DESY. From the comparison some conclusions could be drawn: Kolmogoroff equation is able to describe the evolution of crystallinity also in sheared samples, at least in the conditions analyzed in this work; the evolutions of nucleation rate and spherulitic growth rate, found by tests in which crystallinity did not reach its ultimate value, could be extrapolated to describe tests during which shear was kept until fully crystalline samples were obtained (as done at DESY).

In an attempt of identifying a parameter controlling the effect of flow on crystallization, an Hoffman-Lauritzen equation for the growth rate, whose parameters were identified in a previous work, was assumed to be valid also in flow condition by limiting the effect of flow just on the melting temperature. This flow induced melting temperature could thus be evaluated by the experimental data of growth rate under flow conditions. The undercooling could be thus estimated for each test, and a diagram could be obtained reporting the nucleation rate against the undercooling. It was eventually found that nucleation rate is an exponential function of the undercooling.

References and Notes

(1) Pennings, A. J.; Van der Mark, J. M. A. A.; Booij, H. C. *Colloid Polym. Sci.* **1970**, *236*, 99–111.
(2) Lagasse, R. R.; Maxwell, B. *Polym. Eng. Sci.* **1976**, *16*, 189.
(3) Andersen, P. G.; Carr, S. H. *Polym. Eng. Sci.* **1978**, *18*, 215.
(4) Mackley, M. R.; Keller, A. *Polymer* **1973**, *14*, 16–20.
(5) Keller, A.; Kolnaar, H. W. In *Processing of Polymers*; Meijer, H. E. H., Ed.; VCH: New York, 1997; Vol. *18*, pp 189−268.
(6) Wolkowicz, M. D. *J. Polym. Sci., Polym. Symp.* **1978**, 365–382.
(7) Jerschow, P.; Janeschitz-Kriegl, H. *Rheol. Acta* **1996**, *35*, 127–133.
(8) Vleeshouwers, S.; Meijer, H. E. H. *Rheol. Acta* **1996**, *35*, 391–399.
(9) Kumuraswamy, G.; Issian Ani, M.; Kornfield, J. A. *Macromolecules* **1999**, *32*, 7537–7547.
(10) Pogodina, N. V.; Lavrenko, V. P.; Srinivas, S.; Winter, H. H. *Polymer* **2001**, *42*, 9031–9043.
(11) Seki, M.; Thurman, D. W.; Oberhauser, J. P.; Kornfield, A. J. *Macromolecules* **2002**, *35*, 2583–2594.
(12) Coppola, S.; Balzano, L.; Gioffredi., P. L.; Maffettone, P. L.; Grizzuti, N. P. *Polymer* **2004**, *45*, 3249–3256.
(13) Elmoumni, A.; Waddon, A. J.; Fruitwala, H.; Winter, H. H. *Macromolecules* **2003**, *36*, 6453–6461.
(14) Elmoumni, A.; Winter, H. H. *Rheol. Acta* **2006**, *45*, 793–801.
(15) Van Meerveld, J.; Peters, G. W. M.; Hütter, M. *Rheol. Acta* **2004**, *44*, 119–134.
(16) Balzano, L.; Rastogi, S.; Peters, G. W. M. *Macromolecules* **2008**, *41* (2), 399–408.
(17) Wassner, E.; Maier, R. D. *Proceedings of the XIII International Congress of Rheology*; Cambridge University Press: New York, 2000; Vol. *1*, p 183.
(18) Wunderlich, B. *Macromolecular Physics*; Academic Press: New York, 1970; Vol. *1*.
(19) Janeschitz-Kriegl, H.; Ratajski, E.; Stadlbauer, M. *Rheol. Acta* **2003**, *42*, 355–364.
(20) Monasse, B. *J. Mater. Sci.* **1992**, *27*, 6047–6053.
(21) Haas, T. W.; Maxwell, B. *Polym. Eng. Sci.* **1968**, *9*, 225–231.
(22) Kim, S. P.; Kim, S. C. *Polym. Eng. Sci.* **1993**, *33*, 83–87.
(23) Tribout, C.; Monasse, B.; Haudin, J. M. *Colloid Polym. Sci.* **1996**, *274*, 197–201.
(24) Koscher, E.; Fulchiron, R. *Polymer* **2002**, *43*, 6931–6942.
(25) Huo, H.; Meng, Y.; Li, H.; Jiang, S.; An, L. *Eur. Phys. J.* **2004**, *15*, 167–171.
(26) Tavichai, O.; Feng, L.; Kamal, M. R. *Polym. Eng. Sci.* **2006**, *46* (10), 1468–1475.
(27) Sherwood, C. H.; Price, F. P.; Stein, R. S. *J. Polym. Sci., Polym. Symp.* **1978**, *63*, 77–81.
(28) Godara, A.; Raabe, D.; Van Puyvelde, P.; Moldenaers, P. *Polym. Testing* **2006**, *25*, 460–469.
(29) Eder, G.; Janeschitz-Kriegl, H. In *Materials Science and Technology*; Meijer, H. E. M., Ed.; Wiley Company: New York, 1997; Vol. *18*.
(30) Hwang, W. R.; Peters, G.W. M.; Hulsen, M. A.; Meijer, H. E. H. *Macromolecules* **2006**, *39* (24), 8389–8398.
(31) Van der Beek, M. H. E.; Peters, G. W. M.; Meijer, H. E. H. *Macromolecules* **2006**, *39* (24), 9278–9284.
(32) Mykhaylyk, O. O.; Chambon, P.; Graham, R. S.; Patrick, J; Fairclough, A.; Olmsted, P. D.; Ryan, A. J. *Macromolecules* **2008**, *41*, 1901–1904.
(33) Kamal, M. R.; Lee, O. *Polym. Eng. Sci.* **1999**, *39*, 236–243.
(34) Liedauer, S.; Eder, G.; Janeschitz-Ksriegl, H. *Int. Polym. Process.* **1993**, *3*, 243–250.
(35) Li, L.; de Jeu, W. *Macromolecules* **2004**, *37*, 5646–5652.
(36) Vigny, M.; Tassin, J. F.; Giraud, A.; Lorentz, G. *Polym. Eng. Sci.* **1997**, *37* (11), 1785–1791.
(37) Salem, D. R. *Polymer* **1992**, *33*, 3182–3186.
(38) Vigny, M.; Tassin, J. F.; Lorentz, G. *Polymer* **1999**, *42* (2), 397–401.
(39) Blundell, D. J.; Mahendrasingam, A.; Martin, C.; Fuller, W.; MacKerron, D. H.; Harvie, J. L. *Polymer* **2000**, *41*, 7793–7797.
(40) Chaari, F.; Chaouche, M.; Doucet, J. *Polymer* **2003**, *44* (2), 473–477.
(41) Floudas, G.; Hilliou, L.; Lellinger, D.; Alig, I. *Macromolecules* **2000**, *33*, 6466–6472.
(42) Heeley, E. L.; Gough, T.; Bras, W.; Gleeson, A. J.; Coates, P. D.; Ryan, A. J. *Nucl. Instrum. Methods Phys. Res., Sect. B* **2005**, *238*, 21–27.
(43) Coccorullo, I.; Pantani, R.; Titomanlio, G. *Polymer* **2003**, *44* (1), 307–318.
(44) Pantani, R.; Coccorullo, I.; Speranza, V.; Titomanlio, G. *Polymer* **2007**, *48* (9), 2778–2790.
(45) Pantani, R.; Coccorullo, I.; Speranza, V.; Titomanlio, G. *Prog. Polym. Sci.* **2005**, *30* (12), 1185–1222.
(46) Coccorullo, I.; Pantani, R.; Titomanlio, G. *Int. Polym. Process.* **2005**, *2*, 186–190.
(47) De Santis, F.; Vietri, A. R.; Pantani, R. *Macromol. Symp.* **2006**, *234*, 7–12.
(48) Kumaraswamy, G. *J. Macromol. Sci., Part C: Polym. Rev.* **2005**, *45*, 375–397.
(49) Samuels, R. J. *Structured Polymer Properties*; John Wiley & Sons: New York, 1974.
(50) Murthy, N. S.; Minor, H. *Polymer* **1990**, *31* (6), 996–1002.
(51) Tanner, R.; Qi, F. *J. Non-Newtonian Fluid Mech.* **2005**, *127*, 131–141.
(52) Coppola, S.; Grizzuti, N.; Maffettone, P. *Macromolecules* **2001**, *34*, 5030–5036.
(53) Hoffman, J. D.; Miller, R. L. *Polymer* **1997**, *38* (13), 3151–2112.

MA801524T